

Study on the difference of urban heat island defined by brightness temperature and land surface temperature retrieved by RS technology

Wenxia Qiu^{1, 2}, Huixi Xu^{1, 2}, Zhengwei He^{1*}

¹ Key Laboratory of Geo-special Information Technology, Ministry of Land and Resources, Chengdu University of Technology, Chengdu 610059, China

² Institute of Engineering Surveying, Sichuan College of Architectural Technology, Deyang 618000, China

Received 1 March 2014, www.tsi.lv

Abstract

At present, the Remote Sensing is the most advantage method of studying on the Urban Heat Island (UHI) from the space. In general, the method uses remote sensing images to inverse the brightness temperature or land surface temperature to define the UHI. But have any differences of UHI defined by the two kinds of temperature? And what are the differences? This problem is rarely being studied now. Based on this, the brightness temperature (BT) and the land surface temperature (LST) of the Chengdu City were retrieved using Landsat ETM+ image obtained on July 30, 2006. And then, the differences of UHI defined by the BT and the LST were studied from three aspects, which were temperature value, temperature classification and heat island intensity respectively. Research result are the following: (1) There were some differences between BT and LST, and the variation level of LST was higher than BT. (2) There was a slight difference only on the area covered by the low temperature and the secondary low temperature, and the area covered by the others was equal. Therefore, there was no difference on the area of UHI defined by BT and LST. (3) The UHI intensity defined by LST was slightly higher than that was defined by BT, and the intensity value was determined by the method used.

Keywords: Urban Heat Island (UHI), Brightness Temperature (BT), Land Surface Temperature (LST), Remote Sensing Technology (RS)

1 Introduction

Since Lake Howard discovered the temperature of urban centre in London was higher than that in suburban and proposed the concept of "Urban Heat Island (UHI)" in 1833 [1,2], the research in this area has been intense. The research methods [3] included meteorological data analysis, sit observation, numerical simulation and remote sensing. Above methods, the remote sensing, for large observation range, many times, high-speed, good dynamic performance, low cost, strong spatial response ability, etc, in recent years has become the mainstream method of UHI research [4, 5]. It mainly uses thermal infrared images to inverse the brightness temperature or land surface temperature to study the UHI [6, 7]. Then, have any differences of UHI defined by brightness temperature and land surface temperature? And what are the differences? This problem is rarely being studied now.

Based on this, the brightness temperature and the land surface temperature of study area of the Chengdu city were retrieved, and the difference of UHI defined by them was studied from the temperature value, the temperature grade and the urban heat island intensity, respectively.

2 Research Region and Data Source

The Chengdu City is the capital of the Sichuan Province of China, which is the centre of policy, economy and culture and the hub of communications and transportation in the southwest of China. The longitude of the border is from 102°54' E to 104°53' E, the latitude is from 30°05' N to 31°26' N, and the altitude is from 387 m to 5364 m. In the area, the plain, the hilly area and the mountain area accounts for 40.1%, 27.6% and 32.3%, respectively. The Chengdu city is located in the east of the Chengdu Plain known as "the land of abundance", and the average elevation is 500 m.

The research region is the area within the loop expressway in Chengdu city, its area is 540.83 km². In the region, there are three important ring roads. The First Ring Road was completed in 1987, the Second Ring Road was well versed in 1993, and the Third Ring Road was finished in the end of 2002. The data was Landsat-7 ETM+ image obtained on July 30, 2006, the projection of which was UTM 48N, and the spheroid of which was WGS84. The spatial resolution of the multispectral bands, the thermal infrared band and the panchromatic wave band was 30 m, 60 m and 15 m respectively.

* Corresponding author e-mail: hzw@cdut.edu.cn

3 Data Processing

3.1 RADIATION CALIBRATION

Radiation calibration is a process of converting the digital value (DN) of remote sensing data into spectral radiance value of sensor. For Landsat-7 ETM+ data, the model is formula (1) [8, 9].

$$L_{\lambda} = \frac{L_{\max_{\lambda}} - L_{\min_{\lambda}}}{Q_{\max} - Q_{\min}} (Q_{\lambda} - Q_{\min}) + L_{\min_{\lambda}}, \quad (1)$$

where L_{λ} is the spectral radiance by the sensor ($W \cdot m^{-2} \cdot sr^{-1} \cdot \mu m^{-1}$), Q_{λ} is the digital number of analyzed pixel, Q_{\max} is the maximum digital number (255), Q_{\min} is the minimum digital number, $L_{\max_{\lambda}}$ and $L_{\min_{\lambda}}$ are the maximum and minimum spectral radiance.

3.2 ESTIMATION OF LAND SURFACE EMISSIVITY

The NDVI threshold method [10] proposed by Beck et al. (1990) was adopted to estimate the land surface emissivity, and only the natural surface was considered. If $NDVI < 0.2$, the land surface is considered to be the bare soil. If $NDVI > 0.5$, the land surface is thought to be completely covered by vegetation. And if $0.1 \leq NDVI \leq 0.5$, the land surface is deemed to be covered by vegetation and bare soil mixing. The emissivity of the bare soil and the total vegetation-covered area take the empirical value, which are 0.973 and 0.986 respectively. The bare soil and vegetation mixed coverage area is calculated by formula (2) [11].

$$\begin{aligned} \varepsilon &= \varepsilon_v P_v R_v + \varepsilon_s (1 - P_v) R_s + d_{\varepsilon}, \\ R_v &= 0.92762 + 0.07033 P_v, \\ R_s &= 0.99782 + 0.08362 P_v, \end{aligned} \quad (2)$$

where, ε_v is the vegetation emissivity (0.986), ε_s is the bare soil emissivity (0.973). P_v is the vegetation proportion in pixel, and is estimated by formula (3). d_{ε} is the terrain factors, but it is negligible for the study area located in Chengdu Plain. ρ_s is the surface reflectance acquired in the red and near-infrared band.

$$\begin{aligned} P_v &= \left[\frac{NDVI - NDVI_{\min}}{NDVI_{\max} - NDVI_{\min}} \right]^2 \\ NDVI &= \frac{\rho_{band4} - \rho_{band3}}{\rho_{band4} + \rho_{band3}}. \end{aligned} \quad (3)$$

Considering the NDVI threshold method only for natural surface, the pseudo-colour image of study area,

spatial resolution of which was 15 m, was obtained by the fusion of the image, which was layered by red, green and near-infrared band selected, and the panchromatic wave band. Then, the land surface of study area was divided into three classes, which were the natural surface, the construction surface and the water by the supervised classification method. Thirdly, the NDVI image of study area was masked by the vector data of construction and water surface, the NDVI data of the natural surface was obtained, and so the emissivity of which was obtained by the NDVI threshold method. The emissivity of the construction and water surface was given the empirical value, 0.970 and 0.995 respectively. Finally, the land surface emissivity data of study area (see, Figure1) was generated by overlying the three kinds of images in space.

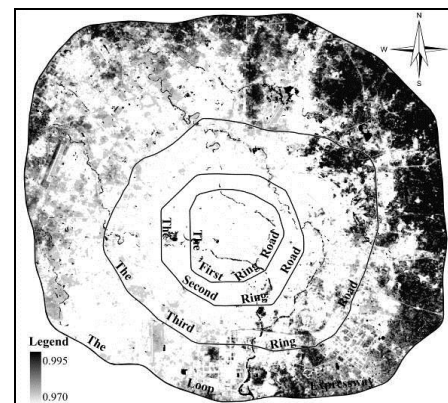


FIGURE 1 Land surface emissivity research region

4 Temperature Inversion

4.1. BRIGHTNESS TEMPERATURE INVERSION

Based on spectral radiation value of pixels on sensor, brightness temperature can be directly calculated by Planck's radiation function or an approximation formula (4) [9, 11, 13] The result is displayed in Figure.2.

$$T_{rad} = K_2 / \ln(1 + K_1 / L_{\lambda}), \quad (4)$$

where T_{rad} is brightness temperature of pixels and its unit is K, K_1 and K_2 are pre-launch calibration constants, K_1 is $666.093 W \cdot m^{-2} \cdot ster^{-1} \cdot \mu m^{-1}$, and K_2 is 1282.708K [14].

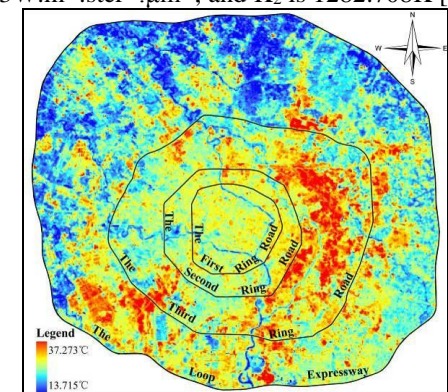


FIGURE 2. Brightness temperature of research region

4.2 LAND SURFACE TEMPERATURE INVERSION

The land surface temperature can be calculated according to formula (5) [9, 15]. And the result is displayed in Figure 3.

$$T_s = \frac{T_{rad}}{1 + (\lambda \cdot T_{rad} / \rho) \ln \epsilon} - 273.15, \quad (5)$$

where, T_s is LST and its unit is $^{\circ}C$, T_{rad} is the brightness temperature and its unit is K, λ is the center wavelength (11.4 μ m), $\rho = h \cdot c / \sigma$, where h is Planck constant ($6.626 \times 10^{-34} J \cdot s$), c is the velocity of light ($2.998 \times 10^8 m/s$), σ is Boltzmann constant ($1.38 \times 10^{-23} J/K$), ϵ is the land surface emissivity.

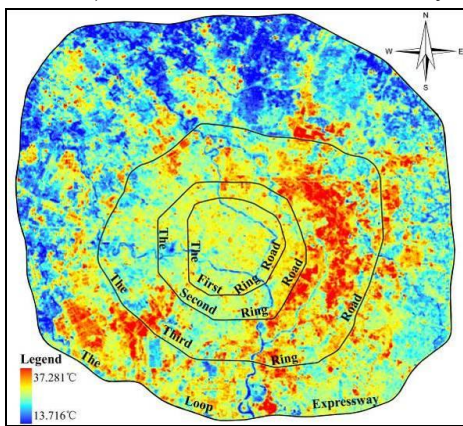


FIGURE 3 Land surface temperature of research region

5 Difference Analysis of UHI

5.1 LAND SURFACE TEMPERATURE INVERSION

According to the statistics from the BT image, the maximum value is 37.273 $^{\circ}C$, the minimum value is 13.715 $^{\circ}C$, the average value is 26.125 $^{\circ}C$, the standard deviation is 1.600. And according to the statistics from the LST, the maximum value is 37.281 $^{\circ}C$, the minimum value is 13.716 $^{\circ}C$, the average value is 26.131 $^{\circ}C$, the standard deviation is 1.601.

By comparison, the characteristic values of the LST are greater than the BT, and the value is from 0.001 $^{\circ}C$ to 0.008 $^{\circ}C$, the average is 0.006 $^{\circ}C$.

5.2 DIFFERENCE ANALYSIS OF TEMPERATURE CLASSIFICATION

Mean-standard deviation method [16] was used to divide temperatures of the research region into five grades, which are high temperature area, secondary high temperature area, medium temperature area, secondary low temperature area and low temperature area. High temperature area and secondary high temperature area are defined as the heat island area; others are called non-heat island area.

From the statistics of the BT classification image, the area of the five grades from high to low temperature respectively was 80.444 km², 85.997 km², 26.158 km², 9.472 km² and 78.759 km², and the UHI area was 166.441 km², accounting for 30.78% of research region. And the statistics from LST classification image showed, the area of the five grades from high to low temperature respectively was 80.444 km², 85.997 km², 226.158 km², 68.124 km² and 80.107 km², and the UHI area was 166.441 km², accounting for 30.78% of research region. From the comparison between the BT classification image and the LST classification image, there was a slight difference only on the area covered by the low temperature and the secondary low temperature, and the area covered by the others was equal. Therefore, there was no difference on the area of UHI defined by BT and LST.

5.3 DIFFERENCE ANALYSIS OF UHI INTENSITY

1) Comparison of the Difference of UHI and non-UHI Average Temperature

The method defines the UHI intensity is the difference between UHI average temperature and non-UHI average temperature. The math model is as the following:

$$P = T_{R,avg} - T_{V,avg}, \quad (6)$$

where P represents heat island intensity, TR, avg is average temperature in UHI area, TV, avg is average temperature in non-UHI area.

By calculation from the BT image, the average temperature of UHI and non-UHI images were 27.9202 $^{\circ}C$ and 25.3271 $^{\circ}C$ respectively, and the UHI intensity was 2.5931 $^{\circ}C$. And statistics from the LST image showed that the average temperature of UHI and non-UHI images were 27.9273 $^{\circ}C$ and 25.3329 $^{\circ}C$ respectively, and the UHI intensity was 2.5944 $^{\circ}C$. Apparently, the UHI intensity defined by LST was 0.0013 $^{\circ}C$ higher than what defined by BT.

2) Heat island area index method

This method used average temperature of non-UHI as basis, define the UHI intensity is the sum of products of the difference between the average temperature of every grade in UHI area and the basis, and its weight, which is the percentage of every grade in UHI area. The math model is formula (7).

$$P = (T_{H,avg} - T_{V,avg}) \times A_H + (T_{SH,avg} - T_{V,avg}) \times A_{SH}, \quad (7)$$

where P represents heat island intensity, TH, avg is the average temperature of high temperature area, TSH, avg is the average temperature of secondary high temperature area, TV, avg is the average temperature of non-UHI area, AH is the weight of high temperature area, ASH is the weight of secondary high temperature area.

The statistics from UHI image defined by BT showed that, the average temperature of high temperature area was 28.6376°C, accounting for 14.87% in UHI area, the average temperature of secondary high temperature area was 27.2492°C, accounting for 15.90%, the average temperature of non-UHI was 25.3271°C, and the UHI intensity calculated by formula (7) was 0.7980°C. And in UHI image defined by LST, the average temperature of high temperature area was 28.6447°C, accounting for 14.87% in UHI area, the average temperature of secondary high temperature area was 27.2561°C, accounting for 15.90%, the average temperature of non-UHI was 25.3329°C, and the UHI intensity calculated was 0.7984°C.

By comparison, the UHI intensity defined by LST was 0.0004°C higher than what defined by BT.

6 Conclusions

Taking the Chengdu City as the research object, the brightness temperature (BT) and the land surface temperature (LST) were retrieved using the Remote Sensing technology, and the difference of the UHI of research region defined by them was researched. The conclusions are as follows:

(1) There were some differences between BT and LST, and the variation level of LST was higher than BT.

References

- [1] Howard L 1833 *Harvey and Darton* 1(3) 1-24
- [2] Matori A, Basith A, Harahap I S H 2012 *Arabian Journal of Geosciences* 5 1069-84
- [3] Liu C, Shi B, Shao Y X, Tang C S 2013 *Bulletin of Engineering Geology and the Environment* 72 303-10
- [4] Cheng F L, Di S, Jiang S D, Jing Y Y, Jun J Z, Dan X 2013 *Arabian Journal of Geoscience* 6(8) 2829-42
- [5] Marialuce S, Marco S 2012 *Computational Science and Its Applications Part II LNCS* 7334 599-608
- [6] Gantuya G, Ji Y H, Young H R, Young Y B 2013 *Journal of Atmosphere Science* 49(4) 535-41
- [7] Petr Dobrovolný 2013 *Theoretical and Applied Climatology* 112 89-98
- [8] Xu H Q 2007 *Geomatics and Information Science of Wuhan University* 32(1) 62-7

(2) There was a slight difference only on the area covered by the low temperature and the secondary low temperature, and the area covered by the others was equal. Therefore, there was no difference on the area of UHI defined by BT and LST.

(3) The UHI intensity defined by LST was slightly higher than that was defined by BT, and the intensity value was determined by the method used.

The above conclusions were based on the remote sensing image of specific phase and specific landscape. If the remote sensing image was different and the study area landform types was different, the results may be different, which need further study.

Acknowledgements

This work was supported in part was supported by the open foundation of the Laboratory of Geo-special Information Technology Ministry of Land and Resources, Chengdu University of Technology China (NO.KLGSIT2013-10), and by the key project of Sichuan Environmental Protection Bureau (NO.2010HBY003), and by the research project of Sichuan College of Architecture Technology (2011) and by Key Project of Education Department of Sichuan Province under Grant 12ZA255 and by The key science and technology project of the Deyang City (NO. 2013ZZ074-05).

- [9] Zhang Y L, Bai Z K, Liu W B 2013 *Geo-Informatics in Resource Management & Sustainable Ecosystem Part I CCIS398* 264-73
- [10] Becker F, Li Z-L 1990 Temperature independent spectral indices in thermal infrared bands *Remote Sensing Environment* 32 17-23
- [11] Qin Z H, Li W, Xu B, Chen Z, Liu J 2004 *Remote Sensing for Land and Resources* 3 28-42
- [12] Mustard J F, Camey M A, Sen A 1999 *Estuarine Coastal and Shelf Science* 49 509-24
- [13] Li C F, Yin J Y, Zhao J J. 2010. *International Journal of Environment Science Development* 3 234-7
- [14] Landsat Project Science Office 2010 *Landsat 7 science data user's handbook*
- [15] Artis D A, Carnahan W H 1982 *Remote Sensing of Environment* 12(4) 313-29
- [16] Chen S L, Wang T X 2009 *Journal of Geo-Information Science* 11(2) 145-7

Authors	
	<p>Wenxia QIU, born on April 18, 1982, Linfen, Shanxi, China</p> <p>Current position, grades: Lecturer University studies: Application of Remote Sensing and GIS Scientific interest: Application of Remote Sensing and GIS Publications: Several articles (EI, Chinese core) Experience: Engaging in teaching and research work at Sichuan College of Architectural Technology, China</p>
	<p>Huixi XU, born in 1979, Deyang, Sichuan, China</p> <p>Current position, grades: Doctor (postdoctor), Associate Professor University studies: Application of Remote Sensing and GIS; Surveying and Mapping Scientific interest: Application of Remote Sensing and GIS; Surveying and Mapping Publications: Several articles (SCI, EI, Chinese core) Experience: Engaging in teaching and research work at Sichuan College of Architectural Technology, China</p>
	<p>Zhengwei HE, born in 1966, South County, Sichuan, China</p> <p>Current position, grades: Doctor(postdoctor), Professor, Doctoral tutor University studies: Remote sensing geology, Ecological Geographic Information System, Ecological environmental geology Scientific interest: Remote sensing geology, Ecological Geographic Information System, Ecological environmental geology. Publications: Several articles (SCI, EI, Chinese core), Several monographs (Chinese, English) Experience: Engaging in teaching and research work in Chengdu University of Technology, China</p>